Available online at www.sciencedirect.com
SCIENCE DIRECT®
Journal of Organometallic Chemistry 689 (2004) 1599–1608
Journal of Organometallic Chemistry
www.elsevier.com/locate/jorganchem

Coordination properties of N_2S (1,5-bis(3,5-dimethyl-1-pyrazolyl)-3-thiapentane) or N_2S_2 (1,8-bis(3,5-dimethyl-1-pyrazolyl)-3,6-dithiaoctane or 1,2-bis[3-(3,5-dimethyl-1-pyrazolyl)-2-thiapropyl]benzene) donor ligands toward Rh(I)

Jordi García-Antón [a,b], René Mathieu [a,*], Noël Lugan [a], Josefina Pons Picart [b,*], Josep Ros [b]

[a] *Laboratoire de Chimie de Coordination du CNRS, 205 Route de Narbonne, 31077 Toulouse Cedex 4, France*
[b] *Departament de Química, Facultat de Ciències – Edifici C sn, Universitat Autònoma de Barcelona, 08193-Bellaterra-Cerdanyola, Barcelona, Spain*

Received 13 January 2004; accepted 10 February 2004

Abstract

The 1,5-bis(3,5-dimethyl-1-pyrazolyl)-3-thiapentane ligand (*bdtp*) reacts with $[Rh(COD)(THF)_2][BF_4]$ to give $[Rh(COD)(bdtp)][BF_4]$ ([**1**][BF_4]), which is fluxional in solution on the NMR time scale. Its further treatment with carbon monoxide leads to a displacement of the 1,5-cyclooctadiene ligand, generating a mixture of two complexes, namely, $[Rh(CO)_2(bdtp)][BF_4]$ ([**2**][BF_4]) and $[Rh(CO)(bdtp\text{-}\kappa^3N,N,S)][BF_4]$ ([**3**][BF_4]). In solution, [**2**][BF_4] exists as a mixture of two isomers, $[Rh(CO)_2(bdtp\text{-}\kappa^2N,N)]^+$ ([**2a**]$^+$) and $[Rh(CO)_2(bdtp\text{-}\kappa^3N,N,S)]^+$ ([**2b**]$^+$; major isomer) rapidly interconverting on the NMR time scale. At room temperature, [**2**][BF_4] easily loses one molecule of carbon monoxide to give [**3**][BF_4]. The latter is prone to react with carbon monoxide to partially regenerate [**2**][BF_4]. The ligands 1,2-bis[3-(3,5-dimethyl-1-pyrazolyl)-2-thiapropyl]benzene (*bddf*) and 1,8-bis(3,5-dimethyl-1-pyrazolyl)-3,6-dithiaoctane (*bddo*) are seen to react with two equivalents of $[Rh(COD)(THF)_2][BF_4]$ to give the dinuclear complexes $[Rh_2(bddf)(COD)_2][BF_4]_2$ ([**4**][BF_4]$_2$) and $[Rh_2(bddo)(COD)_2][BF_4]_2$ ([**5**][BF_4]$_2$), respectively. In such complexes, the ligand acts as a double pincer holding two rhodium atoms through a chelation involving S and N donor atoms. Bubbling carbon monoxide into a solution of [**4**][BF_4]$_2$ results in loss of the COD ligand and carbonylation to give $[Rh_2(bddf)(CO)_4][BF_4]_2$ ([**6**][BF_4]$_2$). The single-crystal X-ray structures of [**3**][CF_3SO_3], [**5**][BF_4]$_2$ and [**6**][BF_4]$_2$ are reported.

Keywords: Rhodium(I); N,S-ligands; Pyrazole; Hemilabile ligands

1. Introduction

The chemistry of transition metal complexes incorporating hemilabile ligands has been widely studied in recent years [1]. The term hemilabile ligand, first introduced by Jeffrey and Rauchfuss [2], refers to polydentate ligands possessing both strong donor groups, anchoring the ligand to the metal centre, and weaker donor groups, which can be more readily displaced from the metal centre, thereby leaving a vacant site or stabilizing transition states. The different types of hemilability have been reviewed by Braunstein and Naud [3].

Pyrazole-containing molecules are attractive potential hemilabile ligands since they are relatively easy to prepare; moreover their steric and electronic properties can be tuned in a straightforward manner [4]. In recent years, we have studied and reported the synthesis and characterization of ligands combining a pyrazolyl group with some other functions containing N (amine) [5], P (phosphine) [6], O (alcohol or ether) [7], and S (thiol or

* Corresponding authors. Tel.: +34935812895; fax: +34935813101.
E-mail addresses: mathieu@lcc-toulouse.fr (R. Mathieu), josefina.pons@uab.es (J. Pons Picart).

0022-328X/$ - see front matter © 2004 Elsevier B.V. All rights reserved.
doi:10.1016/j.jorganchem.2004.02.014

thioether) [8] as donor atoms. In particular, we have investigated the hemilabile properties of the 1,5-bis(3,5-dimethyl-1-pyrazolyl)-3-thiapentane (*bdtp*) and 1,8-bis-(3,5-dimethyl-1-pyrazolyl)-3,6-dithiaoctane (*bddo*) ligands in their association with Pd(II) [8d]. Various examples of *bdtp* coordination to Co(II) [9], Zn(II) [10], Cd(II) [10], Cu(I) [9,11,12] and Ag(I) [9] are available from the literature. The ligand generally acts as tridentate (NSN) – except for [$ZnCl_2$(*bdtp*)], in which it acts as bidentate (NN) – as also observed in our previously reported Pd(II) complexes. On the other hand, *bddo* was previously shown to behave either as bidentate (NN) in Cu(II) and Zn(II) complexes [13,15], or as tretradentate (NSSN) in a Ni(II) complex [15], or even as a *bis*-bidentate NS ligand in a Cd(II) complex [15]. We have found the two first of these coordination modes in the case of Pd(II) [8a].

We have extended this study to Rh(I)/*bdtp* complexes and in this paper the results of our investigations are compared with those recently obtained with Rh(I) complexes of bis[(3,5-dimethyl-1-pyrazolyl)methyl]ethylamine (L_N) [5a] and bis[2-(3,5-dimethyl-1-pyrazolyl)ethyl]ether (L_O) ligands (Scheme 1) [7c]. We also describe the synthesis of the new 1,2-bis[3-(3,5-dimethyl-1-pyrazolyl)-2-thiapropyl]benzene ligand (*bddf*) and the results of our investigation on the bonding properties of both the *bddo* and the *bddf* toward Rh(I).

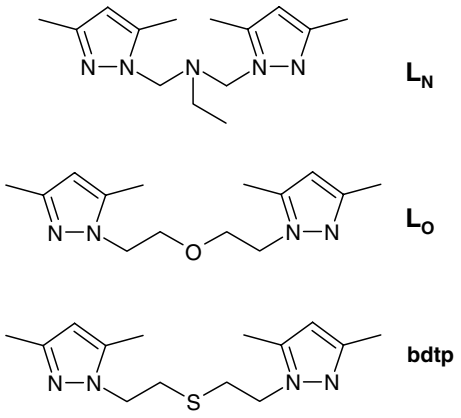

Scheme 1.

2. Results and discussion

2.1. Case of the 1,5-bis(3,5-dimethyl-1-pyrazolyl)-3-thiapentane (bdtp) ligand

The *bdtp* ligand reacts with [Rh(COD)$(THF)_2$][BF_4] – generated *in situ via* reaction of [Rh(COD)Cl]$_2$ with $AgBF_4$ in THF – to give a complex whose elemental analyses are in agreement with the formula [Rh(*bdtp*)(COD)][BF_4] ([**1**][BF_4]). The room temperature ^{1}H NMR spectrum shows sharp resonances for the CH and CH_3 groups of the pyrazolyl cycles, and broad resonances at 4.57 and 4.49 ppm for the NCH_2 group of the *bdtp* ligand and the olefinic hydrogens of the 1,5-cyclooctadiene suggesting the occurrence of a fluxional phenomenon. By lowering the temperature to 183 K, a splitting of the resonances of the CH_3 groups of the pyrazolyl cycle into four somewhat broad signals at 2.55, 2.27, 2.21 and 2.12 ppm is observed. Intricate broad overlapping resonances are observed in the 3–5 ppm region. It is, however, clearly apparent that most of these resonances result from the splitting of the broad resonances observed at room temperature at 4.57 and 4.49 ppm. This shows that the olefinic protons of the 1,5-cyclooctadiene and the NCH_2 protons are no longer equivalent at low temperature. However, the fluxional phenomenon is not frozen at 183 K.

Let us now recall the behavior of the parent Rh(I) complexes of the L_N or L_O ligands (Scheme 1). Two situations have been encountered. In the case of complex [Rh(L_N)(COD)][BF_4], there is a thermodynamic equilibrium in solution between two isomers, one (the minor isomer) in which the ligand is κ^3-bonded and the other one in which the ligand is κ^2-bonded [5a]. For complex [Rh(L_O)(COD)][BF_4], there is only a weak interaction between the rhodium and the oxygen, but the complex is not fluxional [7c]. On this basis, the fluxional behavior of complex [**1**]$^+$ likely results from a combination of two phenomena, namely: (i) a dynamic equilibrium between two isomers in which the ligand *bdtp* would be either κ^2 or κ^3-bonded, which would render the olefinic protons of 1,5-cyclooctadiene non-equivalent at low temperature (Scheme 2) and (ii) a chelate ring-flipping process within the κ^3-bonded isomer, which would render the methy-

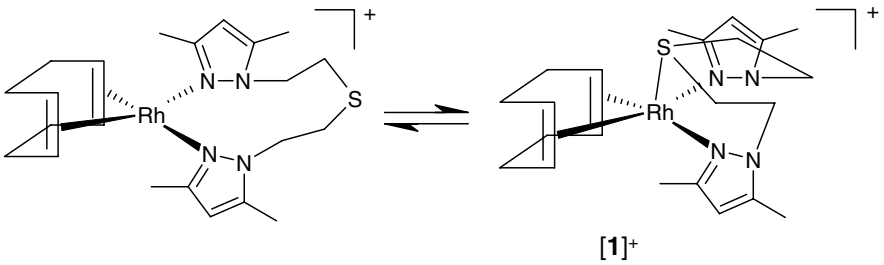

[**1**]$^+$

Scheme 2.

lene and methyl resonances of the *bdtp* ligand magnetically inequivalent.

Bubbling carbon monoxide into a solution of [**1**][BF_4] in dichloromethane at room temperature leads to a mixture of complexes. The infrared spectrum of the solution in the ν(CO) region indeed shows a set of two weak bands at 2103 and 2043 cm^{-1} and a set of two strong bands at 2078 and 2003 cm^{-1} attributable to a first complex, $[\mathbf{2}]^+$, present as a mixture of isomers (vide infra), and a strong band at 2003 cm^{-1} attributable to a second complex, $[\mathbf{3}]^+$. Evaporation of the solution and crystallization led to $[\mathbf{3}]^+$ only as a solid.

The observation of a single peak at 2003 cm^{-1} in the ν(CO) stretching region for $[\mathbf{3}]^+$ is consistent with a κ^3 bonding mode of the *bdtp* ligand. As it was not possible to obtain suitable crystals for an X-ray structure determination, we repeated the reaction with $AgCF_3SO_3$ instead of $AgBF_4$. Suitable crystals of [**3**][CF_3SO_3] could then be obtained. The structure of $[\mathbf{3}]^+$ is shown in Fig. 1 and a list of selected bond distances and angles is given in Table 1. The rhodium atom is bound to the two nitrogen and to the sulfur atoms of the *bdtp* ligand, and also to a carbon monoxide ligand, in a slightly distorted square-planar geometry. The Rh atom lies 0.05 Å above the mean plane formed by the atoms C1, N2, N12 and S1. The Rh–N (2.0432(15) and 2.0454(16) Å) and Rh–C (1.8281(19) Å) bond distances are similar to those found in the [Rh(L_N)(CO)][BPh_4] [5a] and [Rh(L_O)(CO)][BF_4] [7c] complexes, 2.015(3)–2.042(4) Å and 1.795(5)–1.809(4) Å for Rh–N and Rh–C bonds, respectively. No other complex with $RhCN_2S$ core (C carbonyl, S thioether) could be found in the literature. The Rh–S bond distance (2.3938(5) Å) is in the upper limit of the Rh–

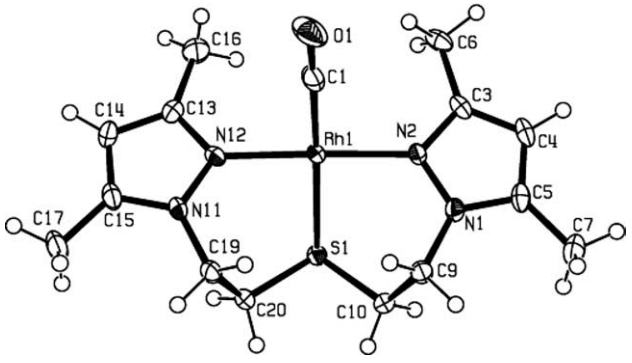

Fig. 1. ORTEP drawing of the cation [Rh(*bdtp*)(CO)]$^+$ ($[\mathbf{3}]^+$) showing the numbering scheme (ellipsoids are shown at the 50% probability level).

Table 1
Selected bond lengths (Å) and angles (°) for $[\mathbf{3}]^+$ with estimated standard deviations in parentheses

$[\mathbf{3}]^+$	
Rh(1)–C(1)	1.828(2)
Rh(1)–N(2)	2.043(2)
Rh(1)–N(12)	2.045 (2)
Rh(1)–S(1)	2.3938(5)
C(1)–Rh(1)–N(2)	92.34(8)
C(1)–Rh(1)–N(12)	90.99(8)
N(12)–Rh(1)–N(2)	176.14(6)
C(1)–Rh(1)–S(1)	172.23(7)
N(12)–Rh(1)–S(1)	87.64(5)
N(2)–Rh(1)–S(1)	89.32(4)

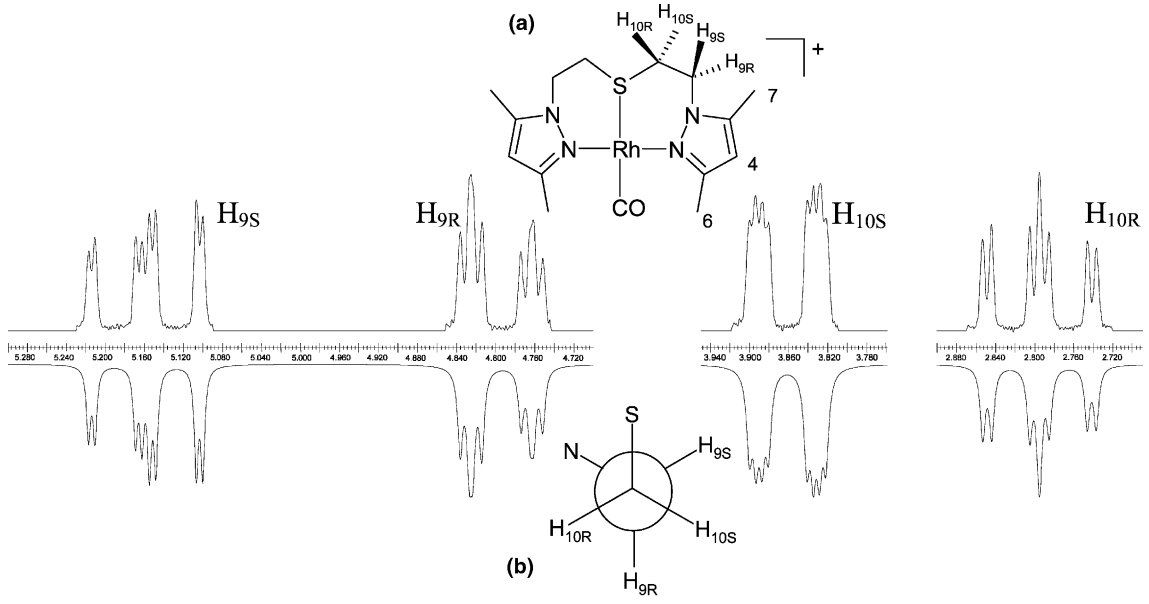

Fig. 2. The 400 MHz ^{1}H NMR (above) and gNMR simulated spectra for the NCH_2CH_2S fragment of [Rh(*bdtp*)(CO)]$^+$ ($[\mathbf{3}]^+$), including (a) the numbering and (b) the dihedral angles for the NCH_2CH_2S fragment.

S(thioether) bonds found in the literature (2.262–2.390 Å range; mean bond distance of 2.322 Å) [16].

The ^{1}H NMR spectrum of $[\mathbf{3}]^+$ in $CDCl_3$ is in agreement with the solid-state structure. The two protons of each CH_2 of the pz–CH_2–CH_2–S chain are diastereotopic, thus leading to four groups of signals (Fig. 2), and each group of signals can be assigned as a doublet of doublets of doublets. This happens due to the rigid conformation of the *bdtp* ligand in its κ^3 bonding mode. This behavior had been previously observed by some of us in similar pyrazole-thioether or pyrazole-thiolate Pd(II) complexes [8]. An HMQC experiment (Fig. 3) was performed to assign protons H_{10R} and H_{10S} to the two doublets of doublets of doublets of lower δ, and H_{9R} and H_{9S} to those of higher δ. NOESY experiments (Fig. 4) allowed us to differentiate H_{9R} from H_{9S} and $CH_3(6)$ from $CH_3(7)$: the singlet that appears at 2.52 ppm shows NOE interaction only with H_4 and was assigned to $CH_3(6)$. The singlet at 2.32 ppm, besides having NOE interaction with H_4, shows strong NOE interaction with the doublets of doublets of doublets at 4.79 ppm and was assigned to $CH_3(7)$. From the X-ray crystal structure (Fig. 1), it can be seen that the nearest proton to $CH_3(7)$ is H_{9R} and therefore it is the one that should present NOE interaction. This information allowed us to assign H_{9R} to the doublets of doublets of doublets at 4.79 ppm, and H_{9S} to the signal at 5.16 ppm. Coupling constants obtained from the gNMR [17] generated ^{1}H NMR simulated spectra (Fig. 2) helped us to differentiate H_{10R} and H_{10S}. These coupling constants agree with the conformation of the S–CH_2–CH_2–N chain as seen in Fig. 1. Geminal ^2J and $\cong 180°$ ^3J coupling constants have indeed significantly higher values than $\cong 30°$ and $\cong 60°$ ^3J coupling constants [18]. Thus, H_{10R} should correspond to the doublet of doublets of doublets at 2.81 ppm and H_{10S} to the one at 3.86 ppm.

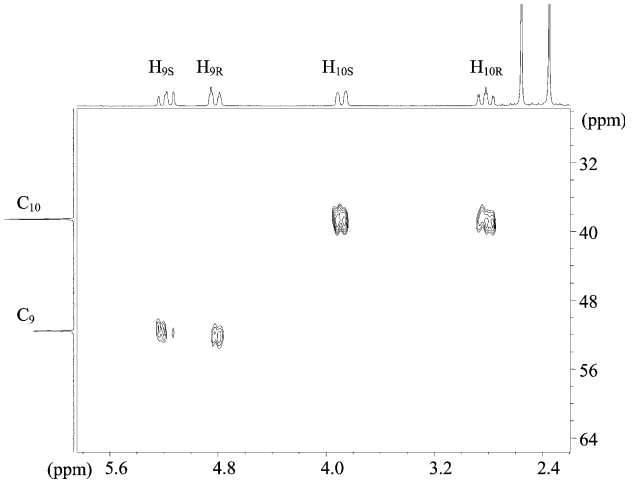

Fig. 3. The 250 MHz 2D HMQC spectrum of [Rh(*bdtp*)(CO)]$^+$ ($[\mathbf{3}]^+$).

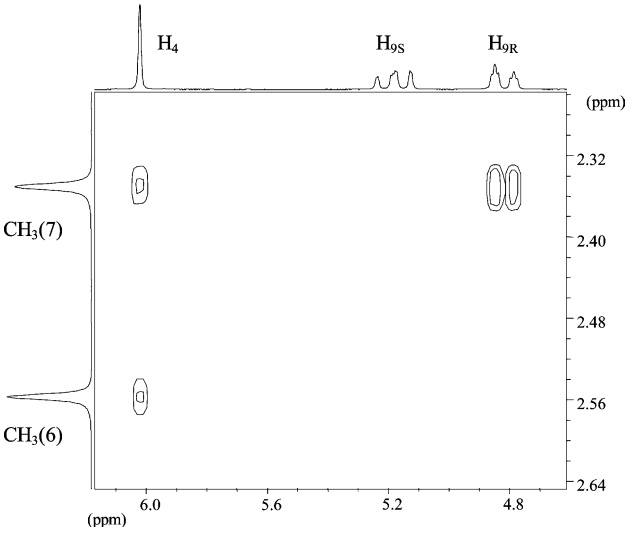

Fig. 4. The 250 MHz 2D NOESY spectrum of [Rh(*bdtp*)(CO)]$^+$ ($[\mathbf{3}]^+$).

Coming back now to the ($[\mathbf{2}][BF_4]$)/($[\mathbf{3}][BF_4]$) mixture in solution, the infrared spectrum shows, in addition to the single band due to $[\mathbf{3}]^+$, two weak absorption bands at 2103 and 2043 cm^{-1} (isomer $[\mathbf{2a}]^+$) and two strong absorption bands at 2078 and 2003 cm^{-1} (isomer $[\mathbf{2b}]^+$). By analogy with the related $[Rh(CO)_2L_N]^+$ and $[Rh(CO)_2L_O]^+$ complexes [5a,7c], we attribute to the minor isomer $[\mathbf{2a}]^+$ a 16 valence-electron structure in which the *bdtp* ligand is κ^2*N*,*N*-bonded to Rh(I), and to the major isomer $[\mathbf{2b}]^+$ a 18 valence-electron isomer with the ligand κ^3*N*,*N*,*S*-bonded to Rh(I). It is worth noting that the $[\mathbf{2a}]^+$/$[\mathbf{2b}]^+$/$[\mathbf{3}]^+$ mixture can be regenerated upon bubbling carbon monoxide through a solution of pure $[\mathbf{3}]^+$ in dichloromethane. However, it is worth noting that even under a carbon monoxide atmosphere, it was not possible to crystallize the di-carbonyl compounds out of the solution.

In addition to the signals due to $[\mathbf{3}]^+$, the 293K ^{1}H NMR spectrum of the $[\mathbf{2a}]^+$/$[\mathbf{2b}]^+$/$[\mathbf{3}]^+$ mixture shows for the CH_2 groups one broad peak at 3.99 ppm and one broad triplet at 3.18 ppm in a 1:1 ratio that gives evidence for a fluxional process in solution. At the same temperature, sharp resonances at 2.27, 2.34, and 6.08 ppm are observed for the methyl and CH groups of the pyrazolyl cycles, respectively. Lowering the temperature to 183 K induces a progressive splitting of the 3.99 ppm resonance into three broad resonances at 4.65, 4.16, and 1.81 ppm, in a 1:2:1 ratio. Concomitantly, the signal at 3.18 ppm splits into four broad resonances at 3.73, 3.19, 2.93, and 2.50 ppm, in the 1:1:1:1 ratio. In the same temperature range, the methyl resonances at 2.27 and 2.34 ppm evolve to give four resonances of equal intensity centred at 2.61, 2.38, 2.16, and 1.69 ppm. There is no significant change observable for the 6.08 ppm resonance, except a slight broadening and a slight shift to 6.03 ppm. From these results it is clear that, as for $[\mathbf{1}]^+$, the fluxional behavior of $[\mathbf{2b}]^+$ implies a conformational equilibrium of the six-membered chelate rings. This is

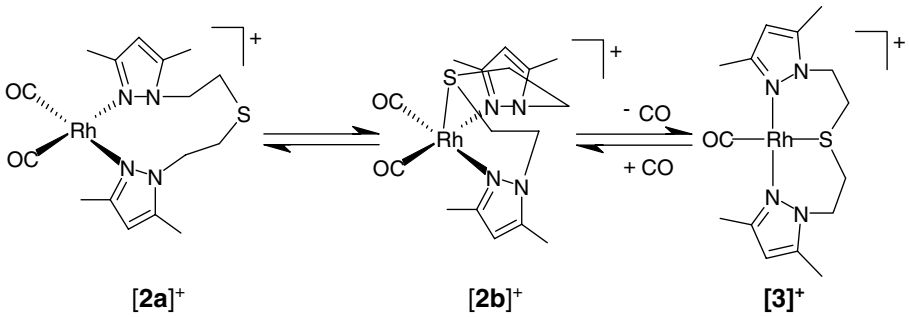

Scheme 3.

corroborated by a low $\Delta G^{\ddagger}$ value of ca. 50 kJ mol^{-1} as deduced from the coalescence behavior of each of the methylene and methyl proton resonances [19]. A similar fluxional behavior has recently been evidenced in a Rh(I) complex of the closely related L_O ligand [7c], and in Pd(II) complexes of tridentate pyrazole-based ligands with a NOS-donor set [8d]. Our observations are summarized in Scheme 3.

In summary, the bonding modes of the *bdtp* ligand, and the L_N and L_O ligands toward Rh(I) are very similar since κ^2 and κ^3 bonding modes have been evidenced in the three complexes. For the dicarbonyl Rh(I) species, in which there is little steric crowding around Rh, the κ^3 bonding mode of the pyrazole-based ligand is the most abundant. In addition, it appears that the $[Rh(bdtp)(CO)_2]^+$ dicarbonyl complex decarbonylates more easily than its L_N and L_O analogues. This is certainly the result of the softer donor character of the sulfur atom compared to nitrogen and oxygen in amine or ether functions. This is supported by the ν(CO) stretching frequency values of the resulting monocarbonyl complexes: 2003 cm^{-1} (*bdtp*), 1997 cm^{-1} (L_N) [5a], 1994 cm^{-1} (L_O) [7c], which decrease with the increase of the hardness of the heteroatom donor centre.

2.2. Case of the 1,2-bis[3-(3,5-dimethyl-1-pyrazolyl)-2-thiapropyl]benzene (bddf) and 1,8-bis(3,5-dimethyl-1-pyrazolyl)-3,6-dithiaoctane (bddo) ligands

The 1,2-bis[3-(3,5-dimethyl-1-pyrazolyl)-2-thiapropyl]benzene (*bddf*) was obtained in good yield by treatment of the lithium thiolate salt of *N*-(2-mercaptoethyl)-3,5-dimethylpyrazole and α,α'-dibromo-*o*-xylene in refluxing tetrahydrofurane (Scheme 4).

The reaction of $[Rh(COD)(THF)_2][BF_4]$ with *bddf* and 1,8-bis(3,5-dimethyl-1-pyrazolyl)-3,6-dithiaoctane (*bddo*) gives, regardless of the initial metal to ligand ratio (from 1:1 to 2:1) is, $[Rh_2(bddf)(COD)_2][BF_4]_2$ ([**4**][BF_4]$_2$) and $[Rh_2(bddo)(COD)_2][BF_4]_2$ ([**5**][BF_4]$_2$), respectively. The room temperature ^{1}H NMR spectra of complexes $[\mathbf{4}]^{2+}$ and $[\mathbf{5}]^{2+}$ are little informative since, except for the sharp resonances of the pyrazolyl cycles, only broad resonances are observed.

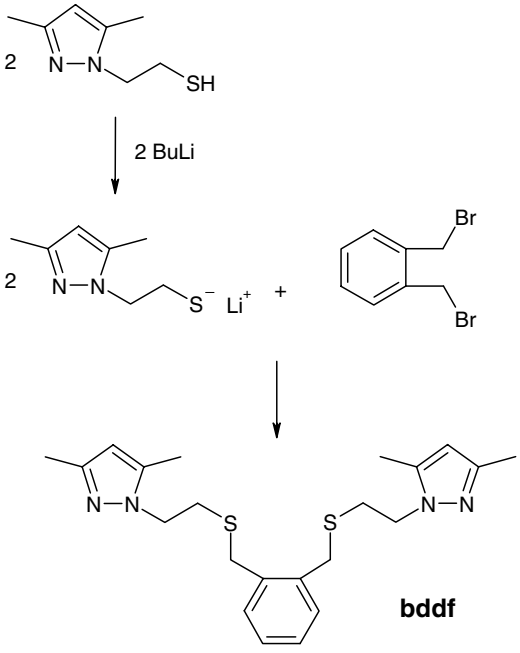

Scheme 4.

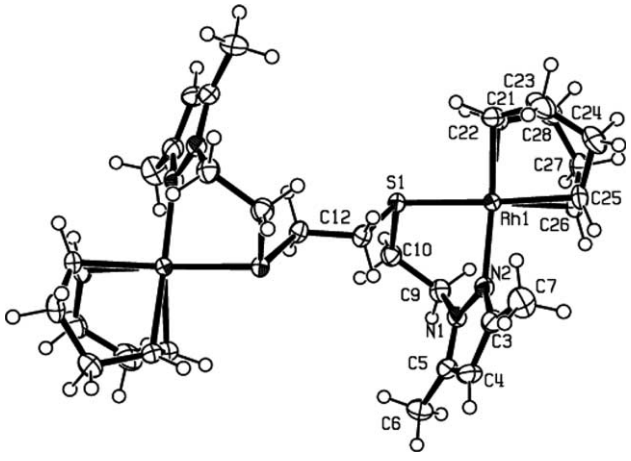

Fig. 5. ORTEP drawing of the cation $[Rh_2(bddo)(COD)_2]^{2+}$ ($[\mathbf{5}]^{2+}$) showing the numbering scheme (ellipsoids are shown at the 50% probability level).

The solid-state structure of [**5**][BF_4]$_2$ was established by X-ray diffraction. It consists of a bimetallic dicationic unit of [Rh_2(*bddo*)(COD)$_2$]$^{2+}$ (Fig. 5) associated with two BF_4^- anions. The cation possesses a crystallographic inversion centre located in the middle of the C12–C12* bond. Each half of the *bddo* ligand is coordinated to a Rh(I) atom through the nitrogen atom of the pyrazolyl ring and the sulfur atom of the thioether group. The coordination sphere of each metal atom is completed by a 1,5-cyclooctadiene ligand. Table 2 lists selected bond distances and angles for [**5**]$^{2+}$. The Rh(I) atom lies 0.057 Å above the mean plane formed by the centroid of C21–C22 and C25–C26 bonds, N2, and S1. The Rh–N (2.092(3) Å) and Rh–S (2.366(2) Å) bond distances are similar to those found in the literature for complexes with Rh–N(pz) (2.015–2.141 Å range; mean bond distance of 2.085 Å) and Rh–S(thioether) (2.262–2.39 Å range; mean bond distance of 2.322 Å), respectively [16].

Attempts to get some insight into the dynamic behavior of complexes [**4**][BF_4]$_2$and [**5**][BF_4]$_2$ by ^{1}H NMR remained inconclusive. Changes in the NMR spectra were indeed observed in the 273 –183 K temperature range but, due to the overlap of the signals, they could not be rationalized.

The solid-state structure of [**5**][BF_4]$_2$ shows that potentially tetradentate N_2S_2 *bddf* and *bddo* ligands act as *bis*-NS bidentate donors in these Rh(I) complexes. A similar coordination mode had previously been encountered in the case of a Cd(II) complex [15]. In other cases, the *bddo* ligand has been found to behave as bridging or *trans* chelating NN ligand (Cu(II), Zn(II) [13–15] or Pd(II) [8a] complexes), or as tetradentate N_2S_2 ligands (Ni(II) [15] and Pd(II) [8a] complexes). In the latter Pd(II) complex, stepwise coordination of the ligand as a tetradentate toward one metal center was found to involve an intermediate bearing two pyrazolyl fragments in *trans* position, followed by isomerization, and coordination of the sulfur atoms, which are weaker donors. The differences observed in the present case may be due to the fact that after coordination of the first pyrazolyl group, the bulky cyclooctadiene ligand blocks the *trans* position, thus preventing the second pyrazolyl ligand to enter the same coordination sphere.

Bubbling carbon monoxide into a solution of [**4**][BF_4]$_2$ gives [Rh_2(*bddf*)(CO)$_4$][BF_4]$_2$ ([**6**][BF_4]$_2$; Scheme 5). A similar reaction carried out from [**5**][BF_4]$_2$ led to the precipitation of an intractable white material. The IR of [**6**]$^{2+}$ shows, in the ν(CO) region, two peaks at 2106 and 2041 cm^{-1} indicating the formation of a dicarbonyl Rh(I) complex. Noticeably, the ν(CO) absorptions bands appear at almost the same frequency as in [**2a**]$^+$.

The structure of [**6**][BF_4]$_2$ was established by an X-ray diffraction study. It consists of a cationic unit of [Rh_2(*bddf*)(CO)$_4$]$^{2+}$ (Fig. 6) associated to two BF_4^- anions. Each half of the *bddf* ligand is coordinated to a Rh(I) atom through one nitrogen of the pyrazolyl cycle and one sulfur of the thioether groups. Two carbonyls ligands in *cis* position complete a slightly distorted square-planar environment around the metal centre. Each Rh(I) centre has 16 valence electrons, consistent with the IR data. Table 2 lists a selection of bond dis-

Table 2
Selected bond lengths (Å) and angles (°) for [**5**]$^{2+}$ and [**6**]$^{2+}$ with esd's in parentheses

[**5**]$^{2+}$		[**6**]$^{2+}$	
Rh(1)–C(21)	2.158(4)	Rh(1)–C(29)	1.91(2)
Rh(1)–C(22)	2.121(4)	Rh(1)–C(30)	1.86(2)
Rh(1)–C(25)	2.174(5)	Rh(2)–C(31)	1.89(2)
Rh(1)–C(26)	2.154(5)	Rh(2)–C(32)	1.86(2)
Rh(1)–N(2)	2.092(3)	Rh(1)–N(2)	2.09(1)
Rh(1)–S(1)	2.366(2)	Rh(2)–N(12)	2.07(1)
		Rh(1)–S(8)	2.38(4)
		Rh(2)–S(18)	2.38(3)
N(2)–Rh(1)–C(22)	154.7(1)	C(30)–Rh(1)–C(29)	89.0(8)
N(2)–Rh(1)–C(26)	95.0(2)	C(30)–Rh(1)–N(2)	170.7(6)
N(2)–Rh(1)–C(21)	167.5(1)	C(29)–Rh(1)–N(2)	94.4(7)
N(2)–Rh(1)–C(25)	95.4(2)	C(30)–Rh(1)–S(8)	89.7(5)
N(2)–Rh(1)–S(1)	86.3(1)	C(29)–Rh(1)–S(8)	172.7(6)
C(22)–Rh(1)–S(1)	93.5(1)	N(2)–Rh(1)–S(8)	88.0(3)
C(26)–Rh(1)–S(1)	149.7(2)	C(32)–Rh(2)–C(31)	85.6(7)
C(21)–Rh(1)–S(1)	90.8(1)	C(32)–Rh(2)–N(12)	177.0(5)
C(25)–Rh(1)–S(1)	173.0(2)	C(31)–Rh(2)–N(12)	93.6(6)
C(22)–Rh(1)–C(26)	97.7(2)	C(32)–Rh(2)–S(18)	90.5(5)
C(22)–Rh(1)–C(21)	37.6(2)	C(31)–Rh(2)–S(18)	175.7(5)
C(26)–Rh(1)–C(21)	81.4(2)	N(12)–Rh(2)–S(18)	90.2(3)
C(22)–Rh(1)–C(25)	82.1(2)		
C(26)–Rh(1)–C(25)	37.1(2)		
C(21)–Rh(1)–C(25)	89.1(2)		

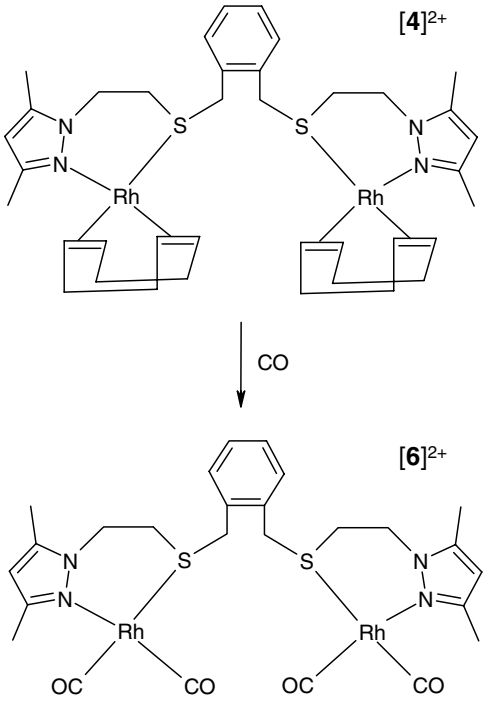

Scheme 5.

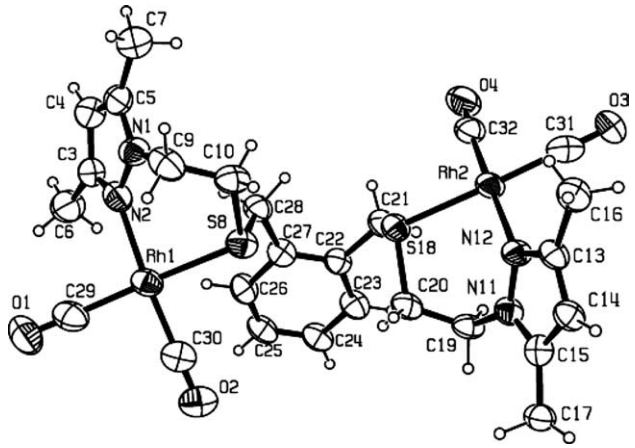

Fig. 6. ORTEP drawing of the cation $[Rh_2(bddf)(CO)_4]^{2+}$ ($[\mathbf{6}]^{2+}$) showing the numbering scheme (ellipsoids are shown at the 30% probability level).

tances and angles. The Rh1 atom lies 0.012 Å above the mean plane formed by the atoms C29, C30, N2 and S8, whereas Rh2 atom lies 0.046 Å above the plane formed by C31, C32, N12 and S18. The Rh–N (2.074(11) and 2.094(13) Å) and Rh–S (2.376(4) and 2.375(3) Å) distances are similar to those found in the parent complex $[\mathbf{5}]^{2+}$ (*vide supra*).

3. Conclusion

This study complements our project aimed at evaluating the bonding properties of N_2X tridentate pyrazolyl-based ligands (X = N, O, S) toward Rh(I). It appears that when no steric strain is imposed by other ligands, these pyrazole-based ligands show a hemilabile character with a good propensity to adopt a κ^3 bonding mode, in equilibrium with a κ^2 bonding mode in low concentration.

The different behavior observed with the *bddf* and *bddo* ligands, both acting as κ^2 N,S ligands toward two Rh(I) centres, is probably the consequence of the presence of the bulky 1,5-cyclooctadiene which remains in the coordination sphere of the metal, thus preventing the κ^2*N*,*N*-bonding mode due to steric crowding.

4. Experimental

4.1. Generals remarks

The syntheses were performed using usual vacuum line and Schlenk techniques. All reagents were commercial grade chemicals and were used without further purification. Diethyl ether, tetrahydrofuran, and dichloromethane solvent used for the syntheses, were dried and distilled by standard methods and stored under nitrogen. 1,5-bis(3,5-dimethyl-1-pyrazolyl)-3-thiapentane (*bdtp*) [8d], bis(3,5-dimethyl-1-pyrazolyl)-3,6-dithiaoctane (*bddo*) [15] and $[RhCl(COD)]_2$ [20] have been prepared according to the published procedures.

Elemental analyses (C, N, H, S) were performed on a Carlo Erba CHNS EA-1108 instrument. Infrared spectra were recorded on a Perkin–Elmer 2000 FT spectrophotometer either in KBr pellets or in CH_2Cl_2 solution in CaF_2 cells. The NMR spectra were obtained on Bruker AC200, WM250, AMX400, or DRX500 instruments. Chemical shifts (δ) were referenced to the residual signals of the deuterated solvent and are given in ppm. Mass spectra were obtained with an Esquire 3000 ion trap mass spectrometer from Bruker Daltonics.

4.2. Synthesis of 1,2-bis[3-(3,5-dimethyl-1-pyrazolyl)-2-thiapropyl]benzene (bddf)

7.2 ml of butyl lithium 1.6 M in hexane (11.5 mmol) were added dropwise to a solution of 1.62 g (10.4 mmol) of *N*-(2-mercaptoethyl)-3,5-dimethylpyrazole in THF (10 ml) keeping the Schlenk flask in an ice-water bath. Precipitation of the lithium thiolate was observed and then 1.41 g (5.1 mmol) of α,α'-dibromo-*o*-xylene 96% in THF (5 ml) were added. The solution was heated under reflux for 5 h. After cooling to room temperature the solvent was evaporated to dryness. Dichloromethane (25 ml) was added and the precipitated LiCl was filtered off. The solution was washed with distilled water (3×20 ml). The organic layer was then dried over anhydrous sodium sulphate and the solvent was removed in vacuum to give *bddf* as a white solid.

bddf: yield: 1.62 g (77%) – $C_{22}H_{30}N_4S_2$ (414.63): C, 63.73; H, 7.29; N, 13.51; S, 15.47. Found: C, 63.58; H, 7.15; N, 13.64; S, 15.73%. IR (KBr, cm^{-1}): $\nu(C–H)_{al}$ 2925, $\nu(C{=}C)$, $\nu(C{=}N)$ 1552, $\delta(C–H)_{oop}$ 780-763. ^1H NMR (250 MHz, $CDCl_3$) $\delta = 2.22$ (s, 12H, 4 *Me*), 2.86 (t, $^3J = 7$ Hz, 4H, S–*CH*$_2$–CH$_2$), 3.64 (s, 4H, S–*CH*$_2$–ph), 4.08 (t, $^3J = 7$ Hz, 4H, pz–*CH*$_2$–CH$_2$), 5.78 (s, 2H, pz–CH), 7.19 (b, 4H, C_6H_4). - $^{13}C\{^1H\}$ NMR (63 MHz, $CDCl_3$) $\delta = 11.3$ (*Me*), 13.6 (*Me*), 32.0 and 33.6 (S–*CH*$_2$–ph and CH$_2$–*CH*$_2$–S), 48.7 (pz–*CH*$_2$–CH$_2$), 105.2 (pz–CH), 127.6–136.2 (C_6H_4), 139.4 and 147.9 (pz–C). MS (ESI): m/z (%) = 415 (100) [M + H^+].

4.3. Synthesis of [Rh(bdtp)(COD)][BF$_4$] ([1][BF$_4$]) and [Rh(bdtp)(COD)][CF$_3$SO$_3$] ([1][CF$_3$SO$_3$])

A solution of 0.081 g (0.416 mmol) of $AgBF_4$ [or 0.107 g (0.416 mmol) of $AgCF_3SO_3$] in methanol (5 ml) was added dropwise and under vigorous stirring to a solution of 0.102 g (0.207 mmol) of $[RhCl(COD)]_2$ in THF (15 ml). The reaction was carried out in the dark to prevent reduction of Ag(I) to Ag(0). The solution turned from an initial orange color to yellow, and AgCl precipitated. After 30 min the solution was filtered through

a Celite pad and 0.116 g (0.417 mmol) of *bdtp* were added. After stirring for 3 h solution was evaporated to dryness and the desired product [**1**][BF_4] [or [**1**][CF_3SO_3]] was crystallized in a dichloromethane/diethyl ether mixture.

[**1**][BF_4]: Yield: 0.219 g (92%) – $C_{22}H_{34}BF_4N_4RhS$ (576.30): C, 45.85; H, 5.95; N, 9.72; S, 5.56. Found: C, 45.63; H, 5.87; N, 9.63; S 5.65%.

[**1**][CF_3SO_3]: Yield: 0.246 g (93%) – $C_{23}H_{34}F_3N_4O_3RhS_2$ (638.57): C, 43.26; H, 5.37; N, 8.77; S, 10.04. Found: C, 43.33; H, 5.25; N, 8.67; S, 9.86%.

[**1**]$^+$: IR (KBr, cm^{-1}): ν(C–H)$_{al}$ 2924, ν(C=C), ν(C=N) 1558, $\nu(CH_3)_{as}$ 1466. ^{1}H NMR (400 MHz, CD_2Cl_2) $\delta = 2.02$ (b, 4H, CH*H*$_{endo}$ COD), 2.28 (s, 6H, *Me*), 2.38 (s, 6H, *Me*), 2.42-2.66 (b, 8H, C*H*H$_{exo}$ COD, pz–CH_2–*CH_2*), 4.49, 4.57 (b, 8H, CH COD, pz–*CH_2*–CH_2), 5.98 (s, 2H, pz–CH). $^{13}C\{^1H\}$ NMR (63 MHz, $CDCl_3$) $\delta = 11.4$ (*Me*), 14.3 (*Me*), 32.3 (b, CH_2 COD), 35.9 (CH_2–*CH_2*–S), 48.6 (pz–*CH_2*–CH_2), 85.7 (b, CH COD), 107.5 (pz–CH), 142.6, 152.2 (pz–C).

4.4. Synthesis of [Rh(bdtp)(CO)$_2$][BF_4] ([**2**][BF_4]) or [Rh(bdtp)(CO)$_2$][CF_3SO_3] ([**2**][CF_3SO_3])

Carbon monoxide was bubbled through a solution of 0.075 g (0.130 mmol) of [**1**][BF_4] or 0.079 g (0.124 mmol) of [**1**][CF_3SO_3] in CH_2Cl_2 (15 ml) for 1 h. The solution was then evaporated to dryness in vacuum to eliminate both the solvent and the COD ligand. The residue was dissolved in CH_2Cl_2 (15 ml) and carbon monoxide was bubbled again. This solution contains a mixture of [**2**]$^+$ and [Rh(*bdtp*)(CO)]$^+$ ([**3**]$^+$) but attempts to isolate the dicarbonyl complexes by crystallization failed even under carbon monoxide atmosphere. The complexes have been identified by IR and NMR spectroscopy, subtracting the data of [**3**]$^+$.

[**2**]$^+$: IR (CH_2Cl_2, cm^{-1}): isomer [**2a**]$^+$ ν(CO) 2103 (w), 2043 (w); isomer [**2b**]$^+$ ν(CO) 2078 (s), 2003 (s). ^{1}H NMR (250 MHz, CD_2Cl_2, 293 K) $\delta = 2.29$ (s, 6H, *Me*), 2.35 (s, 6H, *Me*), 3.18 (b, 4H, CH_2–*CH_2*–S), 3.99 (b, 4H, pz–*CH_2*–CH_2), 6.05 (s, 2H, pz–CH). $^{13}C\{^1H\}$ NMR (63 MHz, $CDCl_3$, 293 K) $\delta = 11.7$ (*Me*), 15.0 (*Me*), 34.9 (CH_2–*CH_2*–S), 47.9 (pz–*CH_2*–CH_2), 107.7 (pz–CH), 144.3, 151.2 (pz–C), 185.0 (d, $^1J = 71.4$ Hz, CO).

4.5. Rh(bdtp)(CO)][BF_4] ([**3**][BF_4]) and [Rh(bdtp)(CO)][CF_3SO_3] ([**3**][CF_3SO_3])

The solution obtained in the preparation of [**2**]$^+$ is evaporated to dryness and [**3**]$^+$ is obtained quantitatively and crystallized in a dichloromethane/diethyl ether mixture.

[**3**][BF_4]: Yield: 0.064 g (99%) – $C_{15}H_{22}BF_4N_4ORhS$ (496.13): C, 36.31; H, 4.47; N, 11.29; S, 6.46. Found: C, 36.25; H, 4.42; N, 11.42; S, 6.33%.

[**3**][CF_3SO_3]: Yield: 0.068 g (98%) – $C_{16}H_{22}F_3N_4O_4RhS_2$ (558.40): C, 34.41; H, 3.97; N, 10.03; S, 11.46. Found: C, 34.58; H, 3.83; N, 10.07; S, 11.21%.

[**3**]$^+$: IR (KBr, cm^{-1}): ν(C–H)$_{ar}$ 3129–3018, ν(C–H)$_{al}$ 2968–2924, ν(CO) 1995, ν(C=C), ν(C=N) 1551, $\delta(CH_3)_{as}$ 1462, δ(C–H)$_{oop}$ 822-793. ^{1}H NMR (250 MHz, $CDCl_3$) $\delta = 2.32$ (s, 6H, *Me*), 2.52 (s, 6H, *Me*), 2.81 (ddd, 2H, CH_2–*CH*H–S, $^2J = 14.7$ Hz, $^3J = 3.3$ Hz, $^3J = 2.2$ Hz), 3.86 (ddd, 2H, CH_2–*CH*H–S, $^2J = 14.7$ Hz, $^3J = 12.1$ Hz, $^3J = 1.6$ Hz), 4.79 (ddd, 2H, pz-*CH*H-CH_2, $^2J = 15.6$ Hz, $^3J = 2.2$, $^3J = 12.1$), 5.16 (ddd, 2H, pz-*CH*H-CH_2, $^2J = 15.6$ Hz, $^3J = 3.3$ Hz, $^3J = 1.6$ Hz), 5.98 (s, 2H, pz–CH). $^{13}C\{^1H\}$ NMR (63 MHz, $CDCl_3$) $\delta = 12.3$ (*Me*), 16.1 (*Me*), 38.7 (CH_2–*CH_2*–S), 51.7 (pz–*CH_2*–CH_2), 108.0 (pz–CH), 143.3, 152.6 (pz–C), 181.8 (d, $^1J = 81.1$ Hz, CO).

4.6. Complexes [Rh$_2$(bddf)(COD)$_2$][BF_4]$_2$ ([**4**][BF_4]$_2$) and [Rh$_2$(bddo)(COD)$_2$][BF_4]$_2$ ([**5**][BF_4]$_2$)

A solution of 0.069 g (0.354 mmol) of $AgBF_4$ in THF (5 ml) was added dropwise and under vigorous stirring to a solution of 0.088 g (0.179 mmol) of [RhCl(COD)]$_2$ in THF (15 ml). The reaction was carried out in the dark to prevent reduction of Ag(I) to Ag(0). Solution turned from an initial orange color to yellow, and AgCl precipitated. After 30 min the solution was filtered through a Celite pad and 0.073 g (0.177 mmol) of *bddf* [or 0.060 g (0.177 mmol) of *bddo*] were added. After stirring for 3 h solution was evaporated to dryness and the desired product [**4**][BF_4]$_2$ [or [**5**][BF_4]$_2$] was crystallized in a dichloromethane/diethyl ether mixture.

[**4**][BF_4]$_2$: Yield: 0.161 g (90%) – $C_{38}H_{54}B_2F_8N_4Rh_2S_2$ (1010.41): C, 45.17; H, 5.39; N, 5.54; S, 6.35. Found: C, 44.90; H, 5.25; N, 5.39; S, 6.02%. IR (KBr, cm^{-1}): ν(C–H)$_{al}$ 2947, ν(C=C), ν(C=N) 1554, ν(B–F) 1057. ^{1}H NMR (200 MHz, CD_2Cl_2) $\delta = 2.32$ (b, 8H, CH_2(COD)), 2.41 (s, 6H, *Me*), 2.64 (s, 6H, *Me*), 4.93 (b, 4H, CH(COD)), 6.14 (s, 2H, pz–CH), 7.63 (b, 4H, C_6H_4). $^{13}C\{^1H\}$ NMR (50 MHz, CD_2Cl_2) $\delta = 12.3$ (*Me*), 16.0 (*Me*), 29.2, 33.6 (b, CH_2(COD)) 36.1, 40.3 (CH_2–*CH_2*–S, S–*CH_2*–ph), 50.3 (pz–*CH_2*–CH_2–S), 82.8, 88.5, 96.0 (b, CH(COD)), 109.8 (pz–CH), 130.4, 132.6, 133.8 (C_6H_4), 144.6, 150.7 (pz–C).

[**5**][BF_4]$_2$: Yield: 0.152 g (92%) – $C_{32}H_{50}B_2F_8N_4Rh_2S_2$ (934.31): C, 41.14; H, 5.39; N, 6.00; S, 6.86. Found: C, 40.88; H, 5.51; N, 5.81; S, 6.68%. IR (KBr, cm^{-1}): ν(C–H)$_{al}$ 2920–2836, ν(C=C), ν(C=N) 1556, ν(B–F) 1054. ^{1}H NMR (200 MHz, CD_2Cl_2) $\delta = 2.17$ (b, 8H, CH*H*$_{endo}$ COD), 2.35 (s, 6H, *Me*), 2.44 (s, 6H, *Me*), 2.50 (b, 12H, C*H*H$_{exo}$ COD, S*CH_2*–*CH_2*S), 3.06 (b, 4H, pz–CH_2–*CH_2*), 4.60 (b, 4H, CH COD), 5.00 (b, 4H, pz–*CH_2*–CH_2), 5.99 (s, 2H, pz–CH). $^{13}C\{^1H\}$ NMR (50 MHz, CD_2Cl_2) $\delta = 12.1$ (*Me*), 15.3 (*Me*), 29.2, 33.7 (b,

CH_2(COD)) 35.6 (pz–CH_2–*CH_2*–S, S–*CH_2*–*CH_2*–S), 50.6 (pz–*CH_2*–CH_2–S), 85.3 (b, CH(COD)), 109.4 (pz–CH), 144.8, 151.2 (pz–C).

4.7. Complex [Rh_2(bddf)(CO)$_4$][BF_4]$_2$ ([**6**][BF_4]$_2$)

Carbon monoxide was bubbled through a solution of 0.075 g (0.074 mmol) of [**4**][BF_4]$_2$ in CH_2Cl_2 (15 ml) for 1 h. The solution was then evaporated to dryness in vacuum to eliminate both the solvent and the COD ligand. The residue was dissolved in CH_2Cl_2 (15 ml) and carbon monoxide was bubbled again. The desired product [**6**][BF_4]$_2$ was crystallized in a dichloromethane/diethyl ether mixture.

[**6**][BF_4]$_2$: Yield: 0.048 g (71%) – $C_{26}H_{30}B_2F_8N_4O_4Rh_2S_2$ (906.09): C, 34.46; H, 3.34; N, 6.18; S, 7.08. Found: C, 34.42; H, 3.25; N, 6.14; S, 7.25. IR (CH_2Cl_2 solution, cm^{-1}): ν(CO) 2105, 2046. IR (KBr, cm^{-1}): ν(C–H)$_{ar}$ 3140–3010, ν(CO) 2106, 2041, ν(C=C), ν(C=N) 1551, ν(B–F) 1056. ^{1}H NMR (200 MHz, CD_2Cl_2 solution) $\delta = 2.41$ (s, 6H, *Me*), 2.52 (s, 6H, *Me*), 3.18 (m, 4H, CH_2–*CH_2*–S), 4.07 (s, 4H, S–*CH_2*–ph), 4.65 (m, 4H, pz–*CH_2*–CH_2), 6.20 (s, 2H, pz–CH), 7.41–7.51 (m, 4H, C_6H_4). ^{13}C{^{1}H} NMR (50 MHz, CD_2Cl_2 solution) $\delta = 11.6$ (*Me*), 15.3 (*Me*), 33.4, 40.4 (CH_2–*CH_2*–S, S–*CH_2*–ph), 49.2 (pz–*CH_2*–CH_2–S), 108.8 (pz–CH), 130.4, 132.0, 132.7 (C_6H_4), 145.6, 152.4 (pz–C), 178.6 (bd, $^1J = 71.0$ Hz, CO), 182.1 (bd, $^1J = 71.0$ Hz, CO).

4.8. X-ray crystallographic study

Crystals of [**3**][CF_3SO_3], [**5**][BF_4]$_2$, and [**6**][BF_4]$_2$ suitable for X-ray diffraction experiments were obtained through re-crystallization from dichloromethane/diethyl ether mixtures. Data were collected on an STOE IPDS diffractometer at 160 K for [**3**][CF_3SO_3] and [**5**][BF_4]$_2$, and at 293 K for [**6**][BF_4]$_2$. Full crystallographic data for the three complexes are gathered in Table 3. All calculations were performed on a personal computer using the WinGX system [21]. The structures were solved by using the SIR-92 program [22], which revealed in each instance the position of most of the non-hydrogen atoms. All remaining non-hydrogen atoms were located by the usual combination of full-matrix least-squares refinement and difference electron density syntheses by using the SHELXL-97 program [23]. Atomic scattering factors were taken from the usual tabulations. Anomalous dispersion terms for Rh atoms were included in F_c. All non-hydrogen atoms were allowed to vibrate anisotropically. All the hydrogen atoms were set in idealized position (R_3CH, C–H = 0.96 Å; R_2CH_2, C–H = 0.97 Å; RCH_3, C–H = 0.98 Å; C(sp^2)–H = 0.93 Å; U_{iso} 1.2 or 1.5 time greater than the U_{eq} of the

Table 3
Crystallographic data for crystal structures [**3**][CF_3SO_3], [**5**][BF_4]$_2$ and [**6**][BF_4]$_2$

Compound	[**3**][CF_3SO_3]	[**5**][BF_4]$_2$	[**6**][BF_4]$_2$
Empirical formula	$C_{16}H_{22}F_3N_4O_4RhS_2$	$C_{32}H_{50}B_2F_8N_4Rh_2S_2$	$C_{26}H_{30}B_2F_8N_4O_4Rh_2S_2$
Molecular mass (g)	558.41	934.31	906.09
T (K)	160(2)	160(2)	293(2)
Crystal system	Triclinic	Monoclinic	Monoclinic
Space group	$P\bar{1}$	$P2_1/c$ (No. 14)	Cc
Unit cell dimensions			
a (Å)	8.8473(5)	9.259(5)	25.531(5)
b (Å)	9.0397(5)	14.021(5)	7.873(5)
c (Å)	14.5691(8)	14.590(5)	17.415(5)
α (°)	103.828(5)		
β (°)	101.877(5)	100.993(5)	96.425(5)
γ (°)	95.474(5)		
V (Å^3)	1094.3(1)	1859.3(14)	3479(3)
Z	2	4	4
D_{calc} (g cm^{-3})	1.695	1.669	1.730
μ (mm^{-1})	1.026	1.070	1.149
F(000)	564	948	1800
Crystal size (mm)	0.5×0.4×0.3	0.1×0.1×0.2	0.4×0.2×0.04
θ range (°)	3.09–30.22	2.03–26.18	2.70–26.09
Reflexions collected			
Total, independent	9636, 5760	14273, 3661	12936, 6581
Data/restraints/parameters	5760/0/275	3661/0/228	6581/2/437
Goodness-of-fit[a]	1.030	0.997	1.003
Final R_1, wR_2	0.0260, 0.0621	0.0383, 0.0732	0.0793, 0.2173
R_1 (all data), wR_2	0.0312, 0.0644	0.0658, 0.0818	0.0949, 0.2390
Residual electron density (e Å^{-3})	0.520 and −1.023	0.532 and −0.427	1.252 and −1.048
Absolute structure parameters			0.06(7)

[a] The function minimized was $\sum w(|F_o|)^2 - |F_c|^2)^2$, where $w = [\sigma^2(I) + (aP)^2]^{-1}$, and $P = (|F_o|^2 + 2|F_c|^2)/3$.

carbon atom to which the hydrogen atom is attached). The final R (on F) factor and ωR (on F^2) values, as well as the numbers of parameters refined and other details concerning the refinement of the crystal structure are presented in Table 3.

5. Supplementary material

CCDC-223820 for [**3**][CF_3SO_3], CCDC-223821 for [**5**][BF_4]$_2$ and CCDC-223822 for [**6**][BF_4]$_2$ contain the supplementary crystallographic data for this paper. These data can be obtained free of charge at www.ccdc.cam.ac.uk/conts/retrieving.html [or from the Cambridge Crystallographic Data Centre, 12 Union Road, Cambridge CB2 1EZ, UK; fax: (internat.) +44-1223-336-033; e-mail: deposit@ccdc.cam.ac.uk].

Acknowledgements

Support by the CNRS and the Spanish Ministerio de Educación y Cultura (Project BQU2000-0238 and a grant to J.G.) is gratefully acknowledged.

References

[1] (a) C.S. Slone, D.A. Weinberger, C.A. Mirkin, Prog. Inorg. Chem. 48 (1999) 233–350;
(b) A. Bader, E. Lindner, Coord. Chem. Rev. 108 (1991) 27–110.
[2] J.C. Jeffrey, T.B. Rauchfuss, Inorg. Chem. 18 (1979) 2658–2666.
[3] P. Braunstein, F. Naud, Angew. Chem. Int. Ed. 40 (2001) 680–699.
[4] (a) S. Trofimenko, Scorpionates: The Coordination Chemistry of Polypyrazolylborate Ligands, Imperial College Press, London, 1999;
(b) S. Trofimenko, Prog. Inorg. Chem. 34 (1986) 115–210;
(c) R. Mukherjee, Coord. Chem. Rev. 203 (2000) 151–218;
(d) P.K. Byers, A.J. Canty, R.T. Honeyman, Adv. Organomet. Chem. 34 (1992) 1–65.
[5] (a) R. Mathieu, G. Esquius, N. Lugan, J. Pons, J. Ros, Eur. J. Inorg. Chem. (2001) 2683–2688;
(b) G. Esquius, J. Pons, R. Yáñez, J. Ros, J. Organomet. Chem. 619 (2001) 14–23;
(c) G. Esquius, J. Pons, R. Yáñez, J. Ros, X. Solans, M. Font-Bardia, J. Organomet. Chem. 605 (2000) 226–233;
(d) G. Esquius, J. Pons, R. Yáñez, J. Ros, X. Solans, M. Font-Bardia, Acta Crystallogr., Sect. C 58 (2002) 133–134;
(e) G. Esquius, J. Pons, R. Yáñez, J. Ros, R. Mathieu, B. Donnadieu, N. Lugan, Eur. J. Inorg. Chem. (2002) 2999–3006.
[6] (a) R. Tribó, J. Pons, R. Yáñez, J.F. Piniella, A. Álvarez-Larena, J. Ros, Inorg. Chem. Commun. 3 (2000) 545–549;
(b) G. Esquius, J. Pons, R. Yáñez, J. Ros, R. Mathieu, B. Donnadieu, N. Lugan, J. Organomet. Chem. 667 (2003) 126–134.
[7] (a) A. Boixassa, J. Pons, A. Virgili, X. Solans, M. Font-Bardia, J. Ros, Inorg. Chim. Acta 340 (2002) 49–55;
(b) A. Boixassa, J. Pons, X. Solans, M. Font-Bardia, J. Ros, Inorg. Chim. Acta 346 (2003) 151–157;
(c) A. Boixassa, J. Pons, J. Ros, R. Mathieu, N. Lugan, J. Organomet. Chem. 682 (2003) 233–239;
(d) A. Boixassa, J. Pons, X. Solans, M. Font-Bardia, J. Ros, Inorg. Chim. Acta 355 (2003) 254–263;
(e) A. Boixassa, J. Pons, X. Solans, M. Font-Bardia, J. Ros, Inorg. Chim. Acta 357 (2004) 733–738.
[8] (a) J. García-Antón, J. Pons, X. Solans, M. Font-Bardia, J. Ros, Eur. J. Inorg. Chem. (2002) 3319–3327;
(b) J. García-Antón, J. Pons, X. Solans, M. Font-Bardia, J. Ros, Inorg. Chim. Acta 355 (2003) 87–94;
(c) J. García-Antón, J. Pons, X. Solans, M. Font-Bardia, J. Ros, Eur. J. Inorg. Chem. (2003) 2992–3000;
(d) J. García-Antón, J. Pons, X. Solans, M. Font-Bardia, J. Ros, Eur. J. Inorg. Chem. (2003) 3952–3957;
(e) J. García-Antón, J. Pons, X. Solans, M. Font-Bardia, J. Ros, Inorg. Chim. Acta 357/2 (2004) 571–580.
[9] W.G. Haanstra, W.L. Driesen, M. van Roon, A.L.E. Stoffels, J. Reddijk, J. Chem. Soc., Dalton Trans. (1992) 481–486.
[10] P. Ghosh, M. Wood, J.B. Bonanno, T. Hascall, G. Parkin, Polyhedron 18 (1999) 1107–1113.
[11] A.L.E. Stoffels, W.G. Haanstra, W.L. Driessen, J. Reedijk, Angew. Chem., Int. Ed. Engl. 29 (1990) 1419–1420.
[12] T.N. Sorrell, M.R. Malachowski, Inorg. Chem. 22 (1983) 1883–1887.
[13] W.G. Haanstra, W.A.J.W. van der Donk, W.L. Driessen, J. Reedijk, J.S. Wood, M.G.B. Drew, J. Chem. Soc., Dalton Trans. (1990) 3123–3128.
[14] W.G. Haanstra, W.L. Driessen, J. Reedijk, J.S. Wood, Acta Crystallogr., Sect. C 48 (1992) 1405–1407.
[15] W.G. Haanstra, W.L. Driessen, J. Reedijk, U. Turpeinen, R. Hämäläinen, J. Chem. Soc., Dalton Trans. (1989) 2309–2314.
[16] F.H. Allen, O. Kennard, Chem. Des. Autom. News 8 (1993) 31–37.
[17] P.H.M. Budzelaar, gNMR ver. 4.0. IvorySoft, Cherwell Scientific, Oxford, 1997.
[18] E. Pretsh, T. Clerc, J. Seibl, W. Simon, Tables of Determination of Organic Compounds: ^{13}C NMR, ^{1}H NMR, IR, MS, UV/Vis, Chemical Laboratory Practice, Springer, Berlin, 1989.
[19] H. Günther, NMR Spectroscopy, Wiley, New York, 1980.
[20] G. Giordano, R.H. Crabtree, Inorg. Synthesis 25 (1990) 88–90.
[21] L.J. Farrugia, J. Appl. Crystallogr. 32 (1999) 837.
[22] A. Altomare, G. Cascarano, C. Giacovazzo, A. Guagliardi, J. Appl. Crystallogr. 26 (1993) 343.
[23] G.M. Sheldrick, SHELXL97: Program for Crystal Structure Analysis (Release 97-2), Institüt für Anorganische Chemie der Universität, Tammanstrasse 4, D-3400 Göttingen, Germany, 1998.